Available online at www.sciencedirect.com
ScienceDirect
Catalysis Today 133–135 (2008) 120–128
CATALYSIS TODAY
www.elsevier.com/locate/cattod

Synthesis, characterization and catalytic behaviour of SAPO-11 obtained at low crystallization times and with low organic agent content

Carmen M. López [a,*], Vanessa Escobar [a], Maria Elena Arcos [b], Leonardo De Nobrega [b], Francisco Yánez [b], Luis V. Garcia [b]

[a] *Universidad Central de Venezuela, Facultad de Ciencias, Escuela de Química, Centro de Catálisis, Petróleo y Petroquímica, Apartado 47102, Caracas 1020-A, Venezuela*
[b] *Universidad Central de Venezuela, Facultad de Ingeniería, Escuela de Ingeniería Química, Apartado 48057, Caracas 1020-A, Venezuela*

Available online 31 January 2008

Abstract

A study of SAPO-11 synthesis using typical compositions of starting gel with low times of crystallization and gels with low proportion of template was carried out. The results show that it is possible to obtain SAPO-11 at short times of crystallization (4 h) with high purity and crystallinity. By decreasing the amount of template of 1–0.3 mol DPA/mol Al_2O_3, it is necessary to change the sources of aluminium and silicon, time and the temperature of crystallization to obtain the phase SAPO-11. In the transformation of 1-butene, a similar behaviour was obtained for SAPO-11 synthesized in the best conditions determined. In the transformation of *n*-pentane over SAPO-11 impregnated with platinum, the best performance was achieved with SAPO-11 obtained at 4 h of crystallization under typical synthesis conditions.

Keywords: Synthesis; SAPO-11; Crystallization

1. Introduction

Silicoaluminophosphate molecular sieves (SAPO) originally reported by Lok et al. [1] have exhibited interesting catalytic properties for acid-catalyzed hydrocarbon transformations [2–5]. These solids have also been used as acidic supports for bifunctional catalysts with a metallic phase for paraffin C_7–C_{15} hydroisomerization reactions [6–8] and for *n*-butane and *n*-pentane dehydroisomerization [9–11]. These sieves are the result of the incorporation of tetravalent silicon (Si^{4+}) into the structure of aluminophosphate molecular sieves. Like the aluminophosphate compositions, SAPO has a variety of structures with pore size ranging between 4 and 8 Å.

SAPO-11 is a silicoaluminophosphate type microporous molecular sieve with AEL structure, consisting of non-intersecting elliptical 10-MR pores of 6.3 × 3.9 Å, orthorhombic crystalline system and typical cell parameters of a = 13.5 Å; b = 18.7 Å; c = 8.45 Å.

Acidity and catalytic properties strongly depend on the silicon content and its occupation in the crystalline network. When silicon atoms are introduced into the frame of a hypothetical $AlPO_4$ structure in the phosphorous sites, which is known as SM2 mechanism, a potential Brönsted site per Si atom is generated. Simultaneous replacement of a pair Al + P atoms by two Si atoms (SM3 mechanism) in combination with mechanism SM2, also yields potential Brönsted acidity. However, the latter leads to less than one acid site per framework Si atom.

The synthesis of the molecular sieves aluminophosphate type takes place through hydrothermal crystallization at autogenous pressure of homogeneous gels containing structural elements. The resulting structure depends on diverse factors, such as nature of the starting materials, composition of the synthesis mixture, and crystallization time and temperature [12]. An organic agent is required for gel preparation, generally an aliphatic amine, which directs synthesis towards a determined structure. In the

* Corresponding author.
E-mail address: cmlopez@ciens.ucv.ve (C.M. López).

0920-5861/$ – see front matter © 2007 Elsevier B.V. All rights reserved.
doi:10.1016/j.cattod.2007.12.093

case of SAPO-11, di-n-propylamine (DPA) is used as an organic agent in the synthesis; a typical composition of a SAPO-11 synthesis gel is Al_2O_3:P_2O_5:0.3SiO_2:DPA:50H_2O, with crystallization at 200 °C during 24 h. The amine to Al_2O_3 and P_2O_5 ratio is 1:1, which approximately represents 30% in weight of amine in the gel. The amine acts as a mould to shape the structure and is trapped in the solid porous structure; then it is eliminated by calcination under air flow.

In previous works in our laboratory, we could obtain SAPO-11 under typical conditions at low crystallization times [13] and in gels with a 0.3:1 amine Al_2O_3 ratio [14]. Furthermore, in synthesis gels for MnAPSO-11 solids, obtained with 1:1 amine/Al_2O_3 ratio, we have determined that the amine retained in the synthesized solid is of the order of 15% in weight [15]; that is, part of the amine remains in the mother solution when the solid is separated after crystallization. This background moved the researchers of this work to prepare and evaluate SAPO-11 catalytically under typical conditions and low crystallization times and in gels with low organic agent content. The decrease of the organic agent content, as well as the low crystallization times, have a positive influence on the economic feasibility of a potential preparation of the solid at a higher scale. The catalytic tests applied were 1-butene skeletal isomerization and *n*-pentane dehydroisomerization.

2. Experimental

2.1. Synthesis and characterization

The following starting materials were used for the synthesis: aluminium hydroxide (AlOH, 53.75% in weight of Al_2O_3 from Aldrich); aluminium isopropoxide (AIP, from Aldrich); orthophosphoric acid (OA from Aldrich); di-*n*-propylamine (DPA, from Aldrich); 40 wt% SiO_2 colloidal silica (Ludox AS-40, from Dupont); 99 wt% SiO_2 precipitated silica designated as Gomasil 200 (G200, from a local company called Venesil), and distilled water as solvent.

To prepare the synthesis gels the source of aluminium was firstly added to a diluted phosphoric acid solution; then the amine and finally the source of silica were subsequently added, at room temperature under vigorous stirring until a homogeneous mixture was obtained. The total stirring time was varied between 3 and 6 h: 1 or 2 h for each step. Gels were transferred into 100 mL Teflon lined stainless-steel autoclaves and heated at 150 or 190 °C (T_c) for crystallization times (t_c) ranging from 0 to 120 h.

The composition of the resulting gels and some other synthesis conditions are given in Table 1. For the experience 1 were used typical synthesis conditions of SAPO-11 [12]; in the experience 2 was varied the gel molar composition by decreasing the amount of DPA. In experience 3, silicon and aluminium sources were changed, as well as the total stirring time and the gel molar composition. The experiences 4 and 5 were carried out under synthesis conditions of experiences 1 and 3, respectively at fixed crystallization time, but using a reactor of 1 L of capacity. The solid products recovered by centrifugation were washed with distilled water and dried at 80 °C overnight. To remove the amine the solids were statically calcined at 500 °C at a heating rate of 5 °C/min with an intermediate stop at 200 °C for 2 h. The samples were named as S-11(*x*;*y* h), where *x* depends on the corresponding experience and *y* is the time of crystallization. For example, S-11(1;4 h) corresponds to the sample obtained in experience 1 after 4 h of crystallization time.

X-ray diffractograms (XRD) of the solid as-prepared were recorded with a Philips diffractometer PW 1730 Phillips using

Table 1
Synthesis conditions used during the preparation of solids

Experience	Gel molar composition	Starting materials	Sample	t_c (h)	T_c °C	% Cryst
1	Al_2O_3:P_2O_5:DPA:0.3SiO_2:50H_2O, total stirring time of 3 h	AlOH	S-11(1;0 h)	0	195	0
		OA	S-11(1;4 h)	4		92
		DPA	S-11(1;12 h)	12		100
		Ludox	S-11(1;24 h)	24		94
2	Al_2O_3:P_2O_5:0.3DPA:0.3SiO_2:50H_2O, total stirring time of 3 h	AlOH	S-11(2;0 h)	0	195	
		OA	S-11(2;4 h)	4		
		DPA	S-11(2;12)	12		
		Ludox	S-11(2;24 h)	24		
3	0.9 Al_2O_3:P_2O_5:0.3DPA:0.1SiO_2:40H_2O, total stirring time of 6 h	IPA	S-11(3;0 h)	0	150	0
		OA	S-11(3;16 h)	16		45
		DPA	S-11(3;24 h)	24		30
		G-200	S-11(3;40 h)	40		
			S-11(3;120 h)	120		
4	Al_2O_3:P_2O_5:DPA:0.3SiO_2:50H_2O, total stirring time of 3 h	AlOH	S-11(4;4 h)	4	195	90
		OA				
		DPA				
		Ludox				
5	0.9 Al_2O_3:P_2O_5:0.3DPA:0.1SiO_2:40H_2O, total stirring time of 6 h	IPA	S-11(5;16 h)	6	150	40
		OA				
		DPA				
		G-200				

Cu Kα radiation operated at 30 kV and 20 mA, and scanning speed of 2° 2θ/min. Diffraction lines between 8 and 25° 2θ/min were taken to determine the degree of crystallinity in the usual way. The sample S-11(1;12 h) with the higher intensity summation of the chosen lines was taken as to be 100% crystalline.

Chemical analysis for Al, P and Si of the calcined samples were performed using atomic emission spectroscopy with a source of plasma inductively coupled. Samples were previously fused with lithium metaborate and dissolved in dilute nitric acid before analyses. N_2-specific surface areas (SSA) were obtained on a Micromeritics 2200 equipment at liquid nitrogen temperature. All the samples were pre-treated at 350 °C under vacuum overnight. Thermogravimetric analysis of the synthesized solids was carried out on a TA Instruments 2100 with SDT 2960 simultaneous d.t.a–t.g.a coupled. Between 20 and 30 mg of the solid was heated at a rate of 10 °C/min under flowing dry air (100 mL/min) from 25 to 900 °C. Scanning electronic microscopy (SEM) micrographs were taken on Hitachi S-500 equipment, operating at 20 keV and 50 mA. The samples were Au-coated for 15 min on an Eiko Engineering instrument.

Surface acidity was characterized by FTIR of the pyridine/solid interaction on a PerkinElmer 1760-X spectrometer. All the spectra in the pyridine region were recorded at room temperature, after outgassing at 250, 350 and 500 °C. The intensity of the bands at 1550 and 1450 cm^{-1} measured after each outgassing temperature, were taken to be proportional to the concentration of Brönsted and Lewis acid sites, respectively. For the purpose of this work three distinct acidity regions were arbitrarily defined in terms of the acid strength: total acidity (weak + moderate + strong) related to those sites retaining pyridine at 250 °C, moderate + strong acidity, ascribed to those sites retaining pyridine at 350 °C and strong acidity, associated with those sites retaining pyridine at 500 °C. Additionally, the total acid site density and the acid strength distribution of the catalysts were measured by temperature programmed desorption of ammonia (TPDA), using a Micromeritics TPD/TPR 2900 analyzer. The total acidity was obtained by integration of the area under the curve. This curve was fitted using two peaks, which were classified as weak and strong acidity depending on the desorption temperature. It was a convenient way to categorize the acid strength distribution obtained by this method.

The Pt-promoted catalysts were prepared by impregnating the calcined solids with $[Pt(NH_3)_4Cl_2]$ (from BDH, reagent grade) using the wet impregnation method with excess solution, to reach 0.5 wt% of Pt. In order to decompose the Pt complex, the catalysts were calcined under a stream of dry air (30 mL/min), the temperature was increased up to 150 °C (5 °C/min) and kept by a 2 h period. The latter was then increased up to 300 °C (5 °C/min) and kept constant for 16 h. The chemisorption measurements were carried out by using a dynamic pulse technique with an argon flow and pulses of H_2. In order to calculate the metal dispersion, and adsorption stoichiometry of metal/H = 1 was assumed. The equipment used was the same as that employed for TPDA.

2.2. Catalytic tests

The transformation of 1-butene was carried out at 400 °C under atmospheric pressure by feeding a mixture of 1-butene/N_2 in a molar ratio of 0.25 to a continuous fixed-bed flow reactor, made of quartz, containing 0.3 g of the catalyst to achieve a weight hourly spatial velocity (WHSV) equal to 1.9 g of 1-butene/(h g of catalyst). Before the reaction, the catalyst is heated under nitrogen stream at 500 °C during 1 h to activate the catalyst. Reaction products are analyzed using a Hewlet-Packard 5890A chromatograph connected in line with the reactor and equipped with a capillary 30 m KCl/Al_2O_3 column and a FID detector.

Since the double bond isomerization of 1-butene is much faster than the skeletal isomerization, the three *n*-butene isomers 1-butene (1B), *cis*-2-butene (*c*2B) and *trans*-2-butene (*t*2B) were considered as reactants in the calculations. Thus, the conversion of 1-butene (X_B) and the selectivity to isobutene (S_{iB}) were defined as follows [16],

$$X_B = \frac{A_{total} - (A_{1B} + A_{c2B} + A_{t2B})}{A_{total}} \times 100 \quad (1)$$

$$S_{iB} = \frac{A_{isobutene}}{A_{total} - (A_{1B} + A_{c2B} + A_{t2B})} \times 100 \quad (2)$$

where A_i is the corrected chromatographic area for a particular compound.

Besides the 1-butene isomers, some lower C_4 products are obtained as well as a small proportion of higher C_4 (<1%) products.

The *n*-pentane transformation was carried out in the same equipment as before, but feeding *n*-pentane by the gas flow saturation method. The feeding gas mixture consisted of N_2 (10 cm^3/min), H_2 (15 cm^3/min) with a partial pressure of *n*-pentane of 0.26 atm. To reach this pressure of *n*-pentane, $H_2 + N_2$ were passed through a glass vessel with *n*-pentane kept to 0 °C in an ice bath. The mass of catalyst was 0.3 g. Before the reaction, a pre-treatment was conducted under nitrogen flow at 500 °C, which was fed through the reactor during 1 h to activate the catalyst. Then N_2 was changed by H_2 which was maintained for 1 h at 500 °C to reduce the metal impregnated in the support. The product analysis was done in the same chromatograph used for the transformation of 1-butene.

The total conversion (X) of *n*-pentane was calculated according to Eq. (3)

$$X = \frac{\sum A_i - A_{n\text{-pentane}}}{\sum A_i} \times 10 \quad (3)$$

For a reaction product, or a set of products, the catalytic yield (Y) is defined by Eq. (4)

$$Y_p = \frac{A_p}{\sum A_i} \times 100 \quad (4)$$

The products were grouped as follows:

Lower C_5 (<C_5) products: adding up the corresponding corrected areas of the C_1–C_4 products, including paraffins and olefins.

Saturated C_5 products (C_5 sat): consisted of *iso*-pentane, neopentane, and cyclopentane.

Non-reacted *n*-pentane: *n*-C_5

Pentenes ($C_5^=$): consisted of the six pentene isomers: 1-pentene, *cis*-2-pentene, *trans*-2-pentene, 2-methyl-2-butene, 2-methyl-1-butene, and 3-methyl-1-butene.

Higher C_5 reaction products ($>C_5$): sum of the corrected areas of C_6–C_8 products.

2.3. Economic study

Costs associated to the starting materials necessary to synthesize 250 g of SAPO-11 were estimated considering the yields obtained in the syntheses carried out. To this end, the amounts of reagents required were calculated in accordance with the compositions of the synthesis gels. Based on these amounts plus the sell prices reported by Aldrich, the production cost of SAPO-11 at laboratory scale, obtained under typical conditions and with low organic agent content was estimated.

3. Results and discussion

3.1. Solid synthesis

Table 1 shows the synthesis experiences carried out upon modification of some parameters of interest to synthesize SAPO-11 under the most favourable conditions that would allow the preparation to be more profitable at a higher scale.

Experience 1 (under typical synthesis conditions of SAPO-11) starts from an amorphous phase (0 h crystallization), and after 4 h of crystallization a high-crystallinity SAPO-11 was obtained. When S-11(1;12 h) was taken as a reference, the proportional crystallinities (% Cryst) of S-11(1;4 h), S-11(1;12 h) and S-11(1;24 h) were ∼92, 100 and 94%, respectively. AEL was the only crystalline phase observed over the range of crystallization time studied. A similar result was obtained in a previous work [13]. The average yield of synthesis was 20%, expressed as grams of solid obtained per 100 g of synthesis gel. This value is similar to the calculated one if the formation of $AlPO_4$ according the following equation:

$$Al(OH)_3 + H_3PO_4 \rightarrow AlPO_4 + 3H_2O \quad \text{yield} : 22\%$$

For the sample at 0 h, a 56% yield is obtained. Considering that according to the gel composition used only 33% in weight of solid can be obtained, the higher value achieved suggests that a solid with amine and occluded water is being formed, as shown by the results of the thermogravimetric analysis presented below.

Fig. 1 shows the changes in the XRD diffractograms of the as-synthesized SAPO-11 obtained in experience 1, with increasing time of crystallization at 195 °C. AEL was the only crystalline phase observed over the whole range of crystallization times studied. The SAPO-11 obtained after 4 h of crystallization was the solid chosen for characterization and catalytic tests, because its preparation should be more profitable due to its short crystallization time.

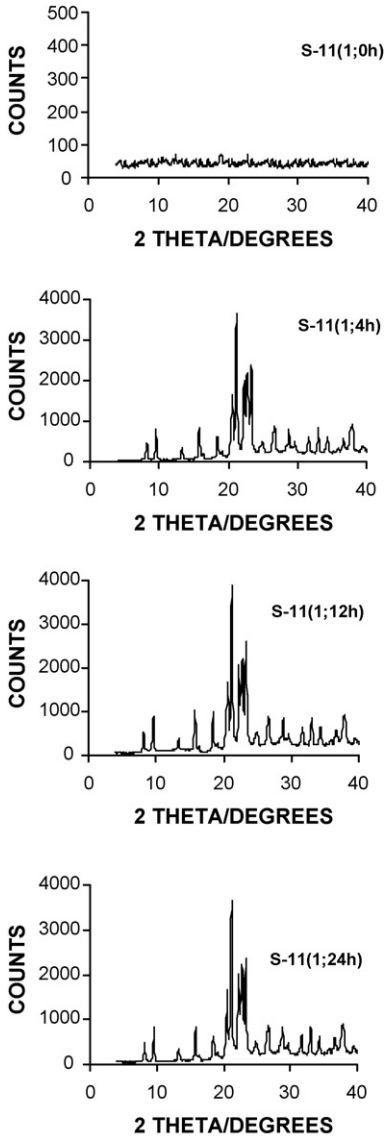

Fig. 1. XRD diffractograms of the as-synthesized SAPO-11 samples with increasing time of crystallization in experience 1.

In second experience, by decreasing the ratio DPA/P_2O_5 to 0.3 and keeping the others synthesis conditions as in experience 1, the dense tridymite phase was obtained for all the crystallization times studied. Fig. 2 shows the DRX pattern of the solid obtained after 12 h.

Experience 3 was conducted following the procedure used in a previous work [14]; in this case, 2-h stirring per stage with a total stirring time of 6 h, was used for the gel preparation. In addition, the gel composition, starting materials, and crystallization temperature were changed. Under these conditions, SAPO-11 was obtained after 16 and 24 h of crystallization, with crystallinity of 45 and 30%, respectively (taking S-11(1;12 h) as reference). These samples had an additional peak at 8.5°, indicating the presence of SAPO-31 phase. The amount of minor crystalline phases was rather small in these samples. At longer times of 24 h, a quite amorphous phase is obtained, which would be indicative of the possible re-dissolution of the solid formed. Fig. 3 shows the XRD diffractograms of the

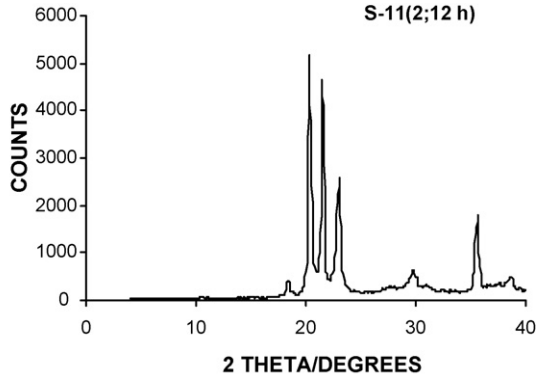

Fig. 2. XRD diffractogram of the sample S-11(2;12 h).

samples obtained in this experience. The sample obtained at 16 h of crystallization was chosen for characterization and catalytic tests; this solid has SAPO-31 as contaminant but its preparation requires a lower proportion of DPA, which can be profitable economically.

A series of attempts to change the synthesis conditions in experience 3 (not showed in this work), such as decreasing stirring time to 1 h per stage, changing the aluminium or silicon source, and decreasing crystallization time, were not successful to obtain SAPO-11; this is consistent with the results presented in reference [14], regarding the narrow synthesis interval to obtain SAPO-11 in gels with a low organic agent content.

Experiences 4 and 5 were carried out with the aim of reproducing at a higher scale in the laboratory, the preparation of S-11(1;4 h) and S-11(3;16 h) solids. These experiences were conducted in a 1 L reactor, using an amount of synthesis gel four times higher in comparison to those used in experiences 1 and 3. The solids obtained exhibited a XRD diffractograms similar to those shown in Figs. 1b, 3b, which demonstrated the synthesis reproducibility at a 4-time higher scale. The evaluated and characterized solids actually correspond to these syntheses.

Table 2 shows the main characteristics of the solids selected after calcination under air flow. For the solids obtained in experience 1, with a starting gel of TO_2 composition equal to $(Al_{0.465}P_{0.465}Si_{0.07})O_2$, the solid formed at 0 crystallization hours contains less silicon than the gel and the results of the chemical analysis show a progressive incorporation of silicon into the solid as crystallization time increases. Solids in experience 2 such as S-11(2;12 h), present low surface areas values and contain silicon; suggesting that the phase obtained is a silicoaluminophosphate with the structure of the dense tridymite phase. A trend similar to that of the solids in experience 1 was observed for solids obtained in experience 3: the phase surface area at 0 h is low and then increases with crystallization time. The SSA and microporous volume of S-11(4;4 h) and S-11(5;16 h) lie within the range previously reported for this kind of solids [15,16]. The sample S-11(5;16 h) with the lower degree of crystallinity showed the lowest adsorption capacity.

The scanning electron micrographs of SAPO-11 catalysts synthesized in experiences 4 and 5 are presented in Fig. 4. The shape of the crystals was spherical being similar to those found

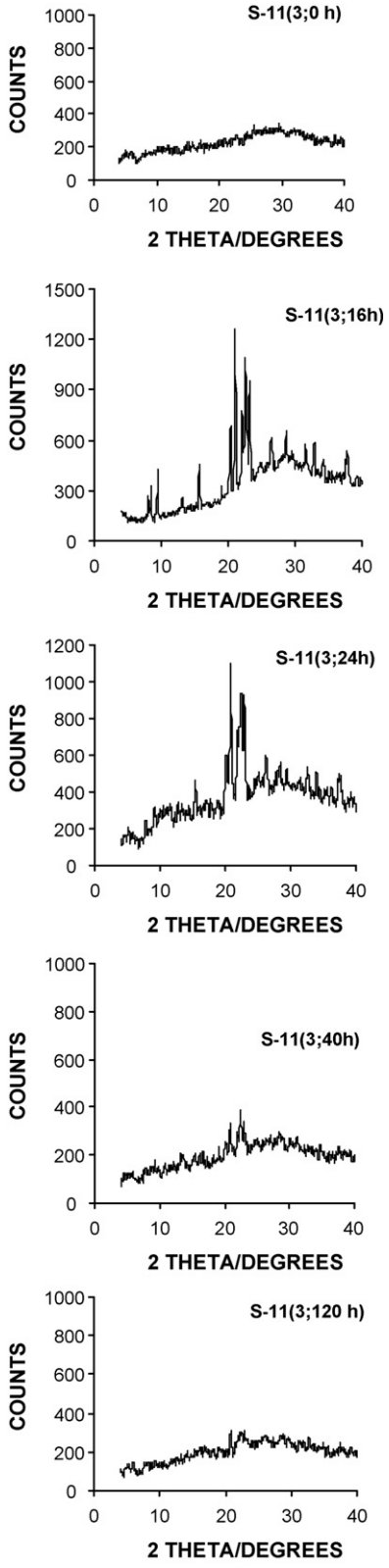

Fig. 3. XRD diffractograms of the as-synthesized SAPO-11 samples with increasing time of crystallization in experience 3.

for SAPO-11 type of microporous materials [15,16]. Crystal size of S-11(4;4 h) was slightly larger than that of S-11(5;16 h).

The results of the thermogravimetric analysis of S-11(4:4 h) and S-11(5;16 h) are shown in Fig. 5. Two weight losses are

Table 2
Specific surface area (SSA), microporous volume (Vp), chemical composition, proportional crystallinity (% Cryst) and the amount (μmol/g) of Brönsted acid sites (BAS) and Lewis acid sites (LAS) after pyridine desorption at 250, 350 and 500 °C

Sample	SSA (m^2/g)	Vp (cm^3/g)	Molar composition formula TO_2	% Cryst	250 °C		350 °C		500 °C	
					BAS	LAS	BAS	LAS	BAS	LAS
S-11(1;0 h)	5	–	$(Al_{0.60}P_{0.36}Si_{0.03})O_2$	0	–	–	–	–	–	–
S-11(4;4 h)	175	0.062	$(Al_{0.50}P_{0.45}Si_{0.05})O_2$	90	12	26	4	11	2	9
S- 11(3;0 h)	10	–	$(Al_{0.53}P_{0.45}Si_{0.03})O_2$	0	–	–	–	–	–	–
S-11(5;16 h)	124	0.044	$(Al_{0.40}P_{0.56}Si_{0.04})O_2$	40	57	55	51	36	50	7
S-11(2;12 h)	15	–	$(Al_{0.49}P_{0.45}Si_{0.06})O_2$	–	–	–	–	–	–	–

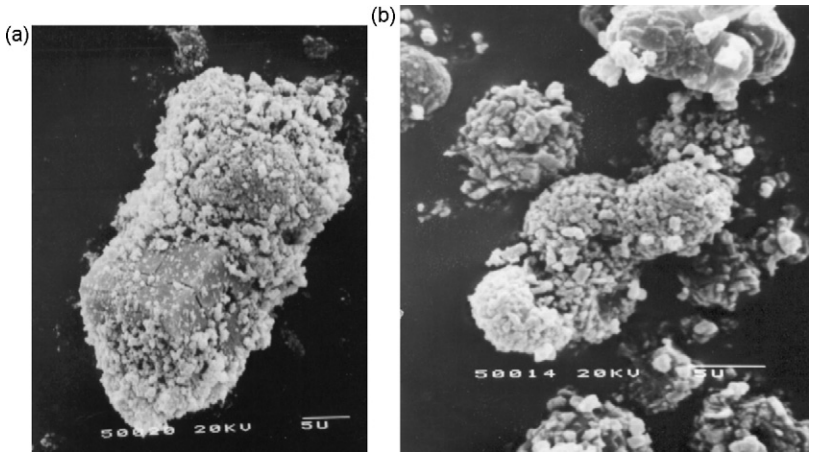

Fig. 4. SEM photographs of samples: (a) S-11(5;16 h) and (b) S-11(4;4 h).

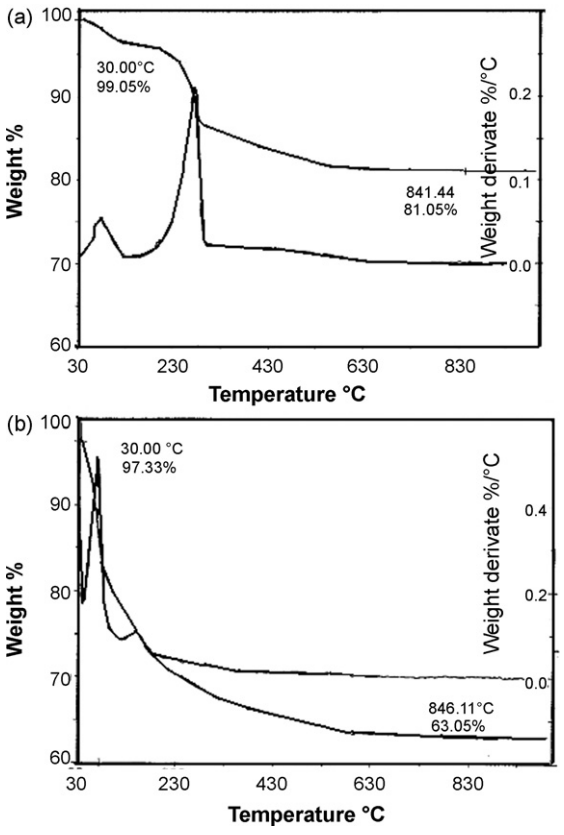

Fig. 5. Thermogravimetric analysis: (a) S-11(4;4 h) and (b) S-11(5;16 h).

observed for S-11(4;4 h) (Fig. 5a): the first one of the order of 3% with a temperature peak at 50° can be due to the adsorbed water; and the second, of the order of 16% and with a temperature peak at 245 °C, is due to the removal of the organic agent; this implies that approximately 12% of the organic agent used in the synthesis mixture should remain in the mother liquor produced in the synthesis. For S-11(5;16 h), in turn, the weight loss amounts to 20%, with a temperature peak at 200 °C. In this case, the weight loss is higher than the amine content in the gel (11%) and it is difficult to determine if the weight loss was due to the water and the occluded amine. Consequently, we think that these two species are combined inside the solid porous structure.

In order to discriminate the weak, moderate and strong acid sites, desorption of pyridine was carried out at 250, 350 and 500 °C, respectively. Integrated areas of the relevant absorption bands are reported in Table 2. The amount of Brönsted acid sites is lower on S-11(4;4 h) compared to S-11(5;16 h), with a high proportion (66%) of sites that retain pyridine up to 250 °C which are considered weak. By contrast for the sample S-11(5;16 h) a high proportion (87%) of sites retaining pyridine up to 500 °C (strong acid sites) was obtained. Lewis acid strength distribution is more comparable on both samples. Observed differences in Brönsted acidity cannot be attributed to variations of the content of silicon in the samples. A possible explanation could be based on differences in synthesis procedure and reagents used, which can influence on location and distribution of silicon in the solids.

Table 3
Acidity data and metal dispersion values of the bifunctional catalysts

Catalyst	D_{H_2} (%)	Surface area (m^2/g_{cat})	Total acidity (mmol NH_3/g_{cat})	Weak acidity (270–350 °C) (mmol NH_3/g_{cat})	Strong acidity (350–500 °C) (mmol NH_3/g_{cat})
S-11(4;4 h)	–	175	0.32	0.25	0.07
S-11(5;16 h)	–	124	0.64	0.50	0.14
Pt/S-11(4;4 h)	40	147	0.29	0.21	0.09
Pt/S-11(5;16 h)	26	80	0.54	0.44	0.10

Table 3 shows acidity data measured by TPDA and metal dispersion values of the catalysts here used. The amount of NH_3 desorbed from the two temperature intervals selected is presented in this Table. As seen, total acidity was 50% higher for S-11(5;16 h) as compared with S-11(4;4 h), in agreement with acidity determined employed FTIR of the pyridine/solid interaction. The addition of platinum decreases the acidity of the catalysts; similar results have been reported on related systems [17]; this decrease was more pronounced over Pt/S-11(5;16 h). It could be possible that a partial blockage of the solid pores occurred when the metal is incorporated. BET surface area values support this hypothesis because lower values of this parameter were obtained in samples with metal; over Pt/S-11(5;16 h) the decrease was bigger than that observed for the Pt/S-11(4;4 h) solid, suggesting a higher stability of SAPO-11 obtained under typical conditions after 4 h of crystallization. According, to this finding, it could be established that the decrease in the strong acid site density with metal incorporation could be due to the acid sites to be partially covered by the metal particles. The Pt dispersion was ~30% larger for the Pt/S-11(4;4 h), compared to that observed for the Pt/S-11(5;16 h) solid, probably due to higher SSA value for the former catalyst.

3.2. Catalytic tests

The synthesized S-11(4;4 h) and S-11(5;16 h) catalysts were tested towards 1-butene isomerization at WHSV of 1.9 h^{-1} and temperature 400 °C. The results are presented in Figs. 6 and 7. The main products were the isomers of *n*-butene (*cis*-2-butene, *trans*-2-butene and isobutene), with low proportions de C_1–C_3 products (propene in higher proportion), isobutane, *n*-butane and pentenes. As can be observed in Figs. 6 and 7, a similar catalytic behaviour was observed. This result shows that the acidity is not directly related to the catalytic activity in case of S-11(5;16 h) and S-11(4;4 h): the amount of Brönsted acid sites is higher over the first sample. Differences in crystallinity and further, distribution of the impure phase as well as differences in location and distribution of the acid sites could be an explanation for these results.

It is worth mentioning that a test was conducted with S-11(2;12 h) with tridymite structure, being obtained a low conversion (2%) with a very low selectivity towards isobutene. This test was carried out to verify the possible activity of this dense phase in the skeletal isomerization of 1-butene; the results show the low activity of this phase, even containing silicon. Tests with $AlPO_4$-11 (without silicon) show less than 1% of yield to isobutene. Therefore, both the AEL structure as well as the presence of silicon in this structure are required for the skeletal isomerization.

n-Pentane catalytic tests were carried out over the S-11(4;4 h) and S-11(5;16 h); the total conversion was always below 2%. The results for the transformation of *n*-pentane over the Pt-promoted solids are shown in Figs. 8–10. A variety of products are produced in the reaction, being the most relevant those lower than C_5 and pentenes. Therefore, the results are presented following the yield variation towards these two groups of products. A low proportion of hydrocarbons (<2%) with more than five carbon atoms were detected. The most striking feature is the decrease in the total conversion and yield for the production of pentenes and C_1–C_4 hydrocarbons, on the Pt/S-11(5;16 h) compared to the Pt/S-

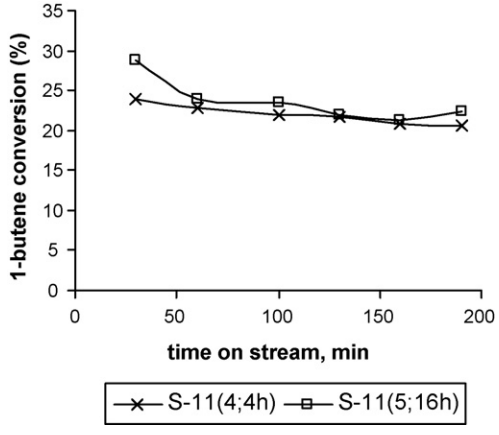

Fig. 6. Total conversion of 1-butene as a function of time on stream measured over evaluated SAPO-11.

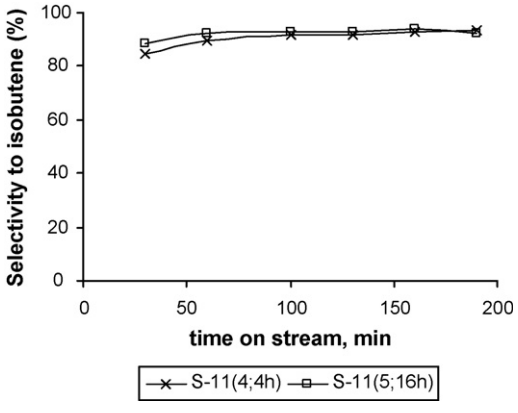

Fig. 7. Selectivity to isobutene as a function of time on stream measured over evaluated SAPO-11.

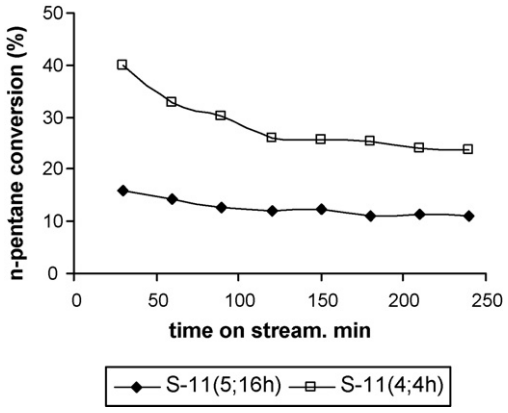

Fig. 8. Total conversion of *n*-pentane as a function of time on stream measured over evaluated SAPO-11.

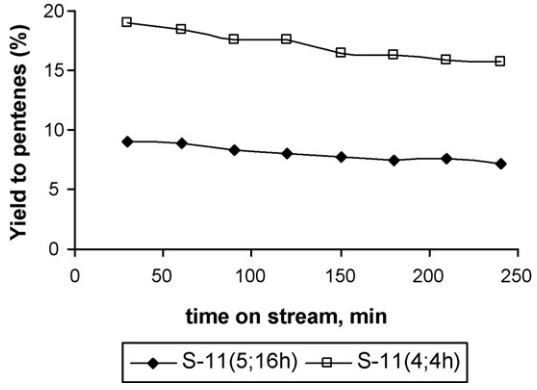

Fig. 9. Yield to pentenes as a function of time on stream measured over evaluated SAPO-11.

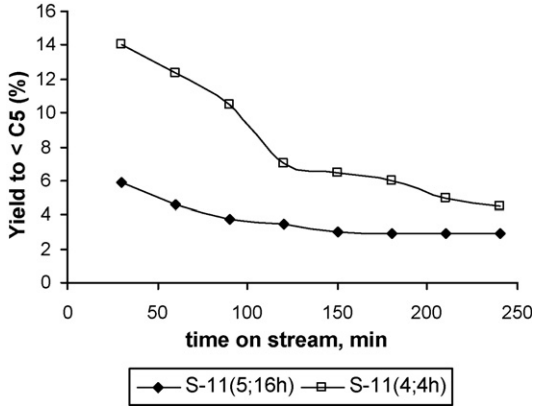

Fig. 10. Yield to lower C_5 products ($<C_5$) as a function of time on stream measured over evaluated SAPO-11.

11(4;4 h) samples. It is worth mentioning that pentene distribution for Pt/S-11(4;4 h) was similar to that given by the thermodynamic equilibrium [18]. These results are consistent with SSA, acidity and dispersion measurements. *n*-Pentane transformation over bifunctional catalysts can take place by a metal assisted process [19]. This mechanism includes: dehydrogenation of *n*-pentane to form *n*-pentenes, skeletal isomerization of the olefin over acid sites to yields *iso*-pentenes, followed by a hydrogenation step to form *iso*-pentenes; the latter is restricted due to high temperature and low pressure of hydrogen. Unwanted side reactions can be occurred [11,19], such as the formation of C_1–C_4 hydrocarbons by the C–C bond breakage on the Pt surface of the Pt/SAPO-11 solids (hydrogenolysis reaction). Since the Pt/S-11(4;4 h) solid has a higher metallic dispersion and SSA, is more active for the productions of *n*-pentenes and subsequently skeletal isomerization of *n*-pentenes is more favoured compared with Pt/S-11(5;16 h) system. Similarly, an increase for the formation of C_1–C_4 hydrocarbons was observed for the Pt/S-11(4;4 h) solid, the global result was a bigger total conversion for this catalyst. It is important to mention that the performance of the Pt/S-11(4;4 h) catalyst obtained after 4 h of crystallization is very similar to that observed for a similar Pt catalyst supported over SAPO-11, obtained after 24 h of crystallization [11].

3.3. Economic study

Costs associated to the raw material required preparing 250 g of SAPO-11 from typical synthesis gels and gels with low content of organic agent, considering solid yield of 24 and 35%, respectively, in the laboratory tests, were estimated. The cost for SAPO-11 of typical composition was $18 and for SAPO-11 with low organic agent content was $14. As expected, when a smaller amount of organic agent is used, the cost is lower. However, some disadvantageous aspects for this preparation have to be taken into consideration: the longer preparation time of the synthesis mixture (6 h vs. 3 h); the longer crystallization time (16 h vs. 4 h); and the specific synthesis conditions regarding the nature of the starting materials, time, and crystallization temperature.

4. Conclusions

SAPO-11 molecular sieves were prepared at low crystallization times under typical conditions and from silicoaluminophosphate gel containing a relatively low DPA concentration without crystal seeding. The latter condition implies a lower cost in raw material, but considerably less flexibility in the preparation. These syntheses are reproducible at two laboratory scales.

The samples of SAPO-11 studied showed high selectivity toward the skeletal isomerization of *n*-butenes. Side reactions, such as oligomerization and cracking were minimized in both samples. The acidity was not directly related to the catalytic activity, however differences in crystallinity, as well as differences in location and distribution of the acid sites could explain these results.

The transformation of *n*-pentane was performed over a platinum-promoted SAPO-11. The higher conversion and yield for the formation of pentenes over Pt/S-11(4;4 h) solid was accounted for in terms of the higher Pt dispersion and surface specific area.

Acknowledgement

This work was financially supported by CDCH-UCV, P.G 03-12-5419-2006.

References

[1] B.M. Lok, C.A. Messina, R.L. Patton, R.T. Gajek, T.R. Cannan, E. Flanigen, U.S. Patent 4,440,871.
[2] J.A. Rabo, R.J. Pellet, P.K. Coughlin, E. Shamshoum, Stud. Surf. Sci. Catal. 46 (1989) 1.
[3] H. Mooiweer, K. de Jong, B. Kraushaar-Czametzki, W. Stork, B. Kruttzen, Stud. Surf. Sci. Catal. 84 (1995) 2327.
[4] L. Gielgens, I. Veestra, V. Ponec, M. Haanepan, J. Van Hooff, Catal. Lett. 32 (1995) 195.
[5] M. Asensi, A. Corma, A. Martínez, J. Catal. 158 (1996) 561.
[6] P. Mériaudeau, V.A. Tuan, G. Splay, V.T. Nghiem, C. Naccache, Catal. Today 49 (1999) 285.
[7] Ch. Geng, F. Zhang, Z. Gao, L. Zhao, J. Zhou, Catal. Today 85 (2004) 93.
[8] S.J. Choung, J.B. Butt, Appl. Catal. A 64 (1990) 173.
[9] A. Vieira, M.A. Tovar, C. Pfaff, P. Betancourt, B. Méndez, C.M. López, F.J. Machado, J. Goldwasser, M.M. Ramírez de Agudelo, Stud. Surf. Sci. Catal. 130 (2000) 269.
[10] A. Vieira, M.A. Tovar, C. Pfaff, P. Betancourt, B. Méndez, C.M. López, F.J. Machado, J. Goldwasser, M.M. Ramírez de Agudelo, M. Houalla, J. Mol. Catal. 101 (1999) 101.
[11] C.M. López, M. De Sousa, Y. Campos, L. Hernández, L. García, Appl. Catal. A 258 (2004) 195.
[12] M. Alfonso, J. Goldwasser, C.M. lópez, F.J. Machado, M. Matjushin, B. Méndez, M.M. Ramírez de Agudelo, J. Mol. Catal. A 98 (1995) 35.
[13] C.M. López, F.J. Machado, B. Méndez, M. Pinto, V. Sazo, J. Goldwasser, M.M. Ramírez de Agudelo, Top. Catal. 10 (2000) 65.
[14] C.M. López, F. Machado, J. Goldwasser, B. Méndez, K. Rodríguez, M.M. Ramírez de Agudelo, Zeolites 19 (1997) 133.
[15] M. Montaño, C. Ramírez, L. García, C.M. López, Revista de la Sociedad Venezolana de Catálisis 15 (2001) 13.
[16] V. Nieminen, N. Kumar, T. Heikkila, E. Laine, J. Villegas, T. Salmi, D. Yu, Appl Catal A 259 (2004) 227.
[17] A. Vieira, M.A. Tovar, C. Pfaff, B. Méndez, C.M. López, F.J. Machado, J. Goldwasser, M.M. Ramírez de Agudelo, J. Catal. 177 (1998) 60.
[18] T. Maurer, B. Kraushaar-Czaretzi, J. Catal. 187 (1999) 202.
[19] G.D. Pirngruber, K. Seshan, J.A. Lercher, J. Catal. 190 (2000) 338.